Perspective Compounds for Immobilization of Spent Electrolyte from Pyrochemical Processing of Spent Nuclear Fuel

Svetlana A. Kulikova [1,*], Sergey S. Danilov [1], Anna V. Matveenko [2], Anna V. Frolova [1], Kseniya Y. Belova [1], Vladimir G. Petrov [2], Sergey E. Vinokurov [1] and Boris F. Myasoedov [1,3]

[1] Vernadsky Institute of Geochemistry and Analytical Chemistry of Russian Academy of Sciences, 19 Kosygin St., 119991 Moscow, Russia; danilov070992@gmail.com (S.S.D.); annav1805@gmail.com (A.V.F.); ksysha_3350@mail.ru (K.Y.B.); vinokurov.geokhi@gmail.com (S.E.V.); bfmyas@mail.ru (B.F.M.)

[2] Department of Chemistry, Lomonosov Moscow State University, 1, bld. 3, Leninskie Gory, 119991 Moscow, Russia; avd.msk11@mail.ru (A.V.M.); vladimir.g.petrov@gmail.com (V.G.P.)

[3] Frumkin Institute of Physical Chemistry and Electrochemistry of Russian Academy of Sciences, 31, bld. 4, Leninsky Prospect, 119071 Moscow, Russia

* Correspondence: kulikova.sveta92@mail.ru; Tel.: +7-495-939-7007

Abstract: Immobilization of spent electrolyte–radioactive waste (RW) generated during the pyrochemical processing of mixed nitride uranium–plutonium spent nuclear fuel is an acute task for further development of the closed nuclear fuel cycle with fast neutron reactors. The electrolyte is a mixture of chloride salts that cannot be immobilized directly in conventional cement or glass matrix. In this work, a low-temperature magnesium potassium phosphate (MPP) matrix and two types of high-temperature matrices (sodium aluminoironphosphate (NAFP) glass and ceramics based on bentonite clay) were synthesized. Two systems ($Li_{0.4}K_{0.28}La_{0.08}Cs_{0.016}Sr_{0.016}Ba_{0.016}Cl$ and $Li_{0.56}K_{0.40}Cs_{0.02}Sr_{0.02}Cl$) were used as spent electrolyte imitators. The phase composition and structure of obtained materials were studied by XRD and SEM-EDS methods. The differential leaching rate of Cs from MPP compound and ceramic based on bentonite clay was about 10^{-5} g/(cm^2·day), and the rate of Na from NAFP glass was about 10^{-6} g/(cm^2·day). The rate of ^{239}Pu from MPP compound (leaching at 25 °C) and NAFP glass (leaching at 90 °C) was about 10^{-6} and 10^{-7} g/(cm^2·day), respectively. All the synthesized materials demonstrated high hydrolytic, mechanical compression strength (40–50 MPa) even after thermal (up to 450 °C) and irradiation (up to 10^9 Gy) tests. The characteristics of the studied matrices correspond to the current requirements to immobilized high-level RW, that allow us to suggest these materials for industrial processing of the spent electrolyte.

Keywords: magnesium potassium phosphate compound; sodium aluminoironphosphate glass; ceramics; bentonite clay; radioactive waste; spent electrolyte; chlorides; immobilization; compressive strength; leaching; thermal stability; radiation stability

1. Introduction

Recently, a combined pyrochemical and hydrometallurgical technology ("PH-process") has been proposed for processing of the mixed uranium–plutonium nitride spent nuclear fuel (MNUP SNF) of the BREST-OD-300 reactor with lead coolant [1]. Pyrochemical processing includes anodic dissolution of the MNUP SNF in a melt of alkali metal chlorides and subsequent cathodic deposition of fissile materials on a liquid cadmium cathode. During this process, a new type of radioactive waste (RW)–spent electrolyte–is produced. This material, as any other types of RW, must be conditioned to obtain a stable (chemically, mechanically, etc.) compound. The choice of a matrix material for the immobilization of such salt waste of a complex chemical composition is not yet obvious, because the activity of the spent electrolyte—of high or medium level—depends on the decontamination factor from the radionuclides of the processed MNUP SNF, and chlorides are difficult to immobilize compounds.

Currently, glass is the only industrial matrix for solidification and immobilization of high-level waste (HLW) used in Russia, Great Britain, Germany, France, USA, China and other countries. Vitrified waste forms have undoubted advantages, first of all, the possibility for continuous control of the technological process, the ability to include various radionuclides, and a relatively high stability. On the other hand, the vitrification is a high temperature process (for phosphate glass (900–1050) °C [2], for borosilicate glass ~1150 °C) [3]), which results in the loss of volatile radionuclides. Moreover, chlorides have the low solubility in glass materials (for example, in borosilicate glass less than 1.5 wt% [4]). Thus, the search for alternative matrix materials that would reliably include and immobilize radioactive chloride waste and other volatile components is an acute task.

The most studied for immobilizing salt waste matrices are the "zeolite/sodalite in glass" systems which are used, for example, in the USA for conditioning of the spent electrolyte from the reprocessing of spent nuclear fuel of the EBR-II reactor [5–9]. Moreover, an alternative method of indirect immobilization was developed by occlusion of a pre-dechlorinated salt waste using a SAP (SiO_2-Al_2O_3-P_2O_5) composite with subsequent solidification in a binder glass [10,11]. Earlier [12,13], a mineral-like titanate matrix, Synrock, was proposed. The main minerals of Synrock are zirconolite, hollandite, perovskite, and rutile. Synroc can be synthesized by hot isostatic pressing and sintering methods. The last was used to produce ceramics for immobilization the Cs and Sr fractions of HLW. The possibility of converting alkali metal chlorides into orthophosphate ceramics was studied by using kosnarite, NZP ($NaZr_2(PO_4)_3$), and langbeinite as matrix materials with addition of NaF as a binder to increase chemical resistance [14]. There is a technology to manufacture fused ceramics that is similar to the production of glassy materials, and a number of works consider murataite as a promising material [15,16]. In the pyrochemical processing of SNF, the murataite matrix is proposed to be used for immobilization of HLW generated during anhydrous reprocessing of SNF of fast neutron reactors, as well as during calcination of solutions used for decontamination of glove boxes and hot cells [16]. In both cases, metal oxides (TiO_2, MnO_2, CaO, Al_2O_3, Fe_2O_3, ZrO_2) were used as the main components to synthesize murataite.

Sodium aluminophosphate (NAFP) glass is a promising matrix for the immobilization of HLW, since its synthesis temperature is lower than that of aluminophosphate glass, which is the only industrial matrix for HLW immobilization used in Russia [2]. Natural clay minerals (bentonite clay) can be used as a possible matrix material for HLW immobilization because the matrix material, in its chemical and phase composition, will be similar to the host rocks of the waste repository [17]. At present, a magnesium potassium phosphate (MPP) matrix, obtained at room temperature and being a synthetic analogue of the natural mineral K-struvite, is considered as an alternative to glass for HLW immobilization. The MPP matrix is an effective mineral-like material with high hydrolytic, mechanical and radiation resistance, as shown earlier in [18–20]. Therefore, these materials were chosen for the immobilization of the spent electrolyte.

The aim of our study was to test the MPP matrix, NAFP glass and ceramics based on bentonite clay as matrix materials for immobilizing imitators of radioactive spent electrolyte, and to determine their physicochemical characteristics, hydrolytic, thermal and radiation stability.

2. Materials and Methods

2.1. Chemicals and Procedures

Various systems are used as electrolytes in industry, including NaCl–2CsCl, NaCl–KCl, LiCl–4.53NaCl–4.88KCl–0.66CsCl, 3LiCl–2KCl and others. The spent electrolyte is contaminated with fission products (primarily Cs, Sr, etc.) and classified as RW, therefore their conversion to stable forms is required [14]. Imitators of the spent electrolyte formed as a result of pyrochemical processing of MNUP SNF with the composition $Li_{0.4}K_{0.28}La_{0.08}Cs_{0.016}Sr_{0.016}Ba_{0.016}Cl$ (25.7 wt% LiCl + 31.6%KCl + 4.1 wt% CsCl + 5.1 wt% $BaCl_2$ + 3.8 wt% $SrCl_2$ + 29.7 wt% $LaCl_3$) [21] and $Li_{0.56}K_{0.40}Cs_{0.02}Sr_{0.02}Cl$ (40 wt% LiCl +

50 wt% KCl + 5 wt% CsCl + 5 wt% $SrCl_2$) [17] were used to synthesize compounds based on MPP matrix, NAFP glass, and bentonite ceramics. The conditions for the synthesis of the studied compounds are presented below.

2.1.1. Synthesis of Low-Temperature MPP Compound

The samples of the MPP compound were prepared at the $MgO:H_2O$ (water content in the RW imitator): KH_2PO_4 weight ratio of 1:2:3 at room temperature. The spent electrolyte imitator solution, which was obtained by dissolving chloride salts in bidistilled water (salt content-554.4 g/L) was solidified. For preparing samples of MPP compounds, MgO (GOST 4526-75, Rushim LLC, Moscow, Russia) were initially pre-precalcined at 1300 °C for 3 h (specific surface area was 6.6 m^2/g) and KH_2PO_4 (TU 6-09-5324-87, Chimmed LLC, Moscow, Russia) crushed to a particle size of 0.15–0.25 mm. Compounds containing up to 12 wt% of the spent electrolyte imitator were obtained. The samples of MPP compound obtained by solidification of aqueous solutions of the spent electrolyte imitator and containing 23 wt% of zeolite (hereinafter the samples are named MPP-Z) were also synthesized. The natural zeolite of the Sokyrnytsya deposit, Transcarpathian region (TU 2163-004-61604634-2013, ZEO-MAX LLC, Ramenskoye, Moscow region, Russia) with a particle size of 0.07–0.16 mm and a specific surface area of 17.5 m^2/g was used for increasing the mechanical strength of the MPP compound just as in the previous work [19].

To study the hydrolytic stability of the MPP compound, samples were also prepared by solidification of the imitator solution containing ^{137}Cs, ^{152}Eu and ^{239}Pu with a specific activity of 6.9×10^7, 2.8×10^7 and 1.8×10^9 Bq/L, respectively. The salts of potassium hexacyanoferrate(II) trihydrate $K_4[Fe(CN)_6] \cdot 3H_2O$ (GOST 4207–75, "Chimmed" LLC, Moscow, Russia) and nickel(II) nitrate hexahydrate $Ni(NO_3)_2 \cdot 6H_2O$ (GOST 4168–79, "JSC Reahim" LLC, Moscow, Russia) were added to solidifying solution imitator in an amount of 1.18 and 0.82 wt%, respectively, for the preliminary binding of cesium cations in $K_xCs_{1-x}Ni[Fe(CN)_6]$ (FKCN) as previously shown in [20].

The obtained mixture was placed in fluoroplastic molds measuring $2 \times 2 \times 2$ cm or $3 \times 1 \times 1$ cm and left for at least for 14 days to set the strength of the compound.

2.1.2. Synthesis of NAFP Glass

The samples of NAFP glass with the composition, mol%: 40Na_2O-10Al_2O_3-10Fe_2O_3-40P_2O_5, which has high crystallization and hydrolytic stability [22–24], were synthesized with 10 wt% of the spent electrolyte imitator in the form of dry salts. The samples were synthesized by melting up to 1200 °C in quartz crucibles with isothermal holding of the resulting melts for 1 h and then pouring onto a metal sheet for glass quenching. Glass batch was prepared from a mixture of dry components $(NH_4)_2HPO_4$ (GOST 3772-74), Na_2CO_3 (GOST 4530-76) Al_2O_3 (TU 6-09-426-75), Fe_2O_3 (TU 6-09-5346-87) (Lenreactive, Saint Petersburg, Russia).

To study the hydrolytic stability of NAFP glass, the samples were prepared containing radioactive tracers ^{137}Cs, ^{152}Eu, and ^{239}Pu. Isotope specific activity of the samples were 2.0, 0.04, and 2.3 MBq/g, respectively.

2.1.3. Synthesis of High-Temperature Ceramics Based on Bentonite

Samples of ceramics based on bentonite clay were obtained by sintering mixture of dehydrated chloride salts (40 wt% LiCl + 50 wt% KCl + 5 wt% CsCl + 5 wt% $SrCl_2$) with bentonite clay (Republic of Khakassia, Russia). Mass ratio of the mixture of salts to bentonite clay was 1:4. Chemical composition of the used bentonite clay, wt%: SiO_2-59.68, CaO-2.76, Al_2O_3-18.63, MgO-2.43, Fe_2O_3-3.93, TiO_2-0.59, Na_2O-0.98, K_2O-1.62. Mineral composition, wt%: montmorillonite–77.1, kaolinite–0.7, quartz–13.3, microcline–3.3, albite–4.9, calcite–0.7 [25]. The synthesis of the samples was performed according to [17]. The mixture of chlorides was ground, dehydrated in an oven at 250 °C for 2 h, and then stored in a desiccator over P_2O_5. All the samples were prepared by mixing and grinding chlorides with the bentonite clay, then the mixture was dried at 100–150 °C and pressed into tablets

with a diameter of 10 mm and a height of 2–4 mm or 8–10 mm using a hand hydraulic press. The last two stages of temperature treatment, the parameters of which were determined in additional studies, were performed in a muffle furnace: the samples were first dried at 400 °C for 4 h, ground again and pressed into tablets for better homogeneity, and then were annealed for 12 h at 900 °C (below the sintering temperature of pure bentonite). The ceramics samples contained 20 wt% of spent electrolyte imitator of the composition $Li_{0.56}K_{0.40}Cs_{0.02}Sr_{0.02}Cl$ were synthesized.

2.2. Methods

The phase composition of the obtained samples was identified by the X-ray diffraction (XRD) method using a diffractometers Ultima-IV (Rigaku, Tokyo, Japan) and Empyrean (Panalytical, Malvern, UK). The XRD data were interpreted using the Jade 6.5 program package (MDI, Livermore, CA, USA) with PDF-2 powder database and the HighScore Plus program. The microstructure of the samples was investigated by the scanning electron microscopy (SEM) using a microscopes Mira3 (Tescan, Brno, Czech Republic) and JEOL JSM-6480LV (JEOL, Tokyo, Japan), the electron probe microanalysis of the samples was performed by energy-dispersive X-ray spectroscopy (EDS) using an analyzer X-Max (Oxford Inst., High Wycombe, UK).

The degree of inclusion of chlorides in NAFP glass was studied using an X-ray fluorescence spectrometer (XRF) Axious Advanced PW 4400/04 (PANalytical B.V., Almelo, The Netherlands).

The compressive strength of the samples of MPP compounds and ceramics based on bentonite clay was determined using a test machine Cybertronic 500/50 kN (Testing Bluhm & Feuerherdt GmbH, Berlin, Germany).

Thermal stability of the samples, obtained after solidification of the spent electrolyte imitators, was investigated in accordance with the current requirements [26] for solidified HLW. This treatment includes heating to 450 °C for 4 h as simulation of thermal heating of materials due to the radioactive decay of alpha-emitters present in HLW. Earlier [21], it was shown that heat treatment at a temperature of ≥ 300 °C resulted in thermal decomposition of the formed FKCN. Thus, the thermal stability of the MPP compound was studied at 270 °C for 4 h. The samples of the MPP compound were preliminarily kept at 180 °C for 10 h for removal of bound water from $MgKPO_4 \cdot 6H_2O$-based compounds in a muffle furnace SNOL 30/1300 (AB UMEGA GROUP, Utena, Lithuania), as previously shown in [18].

The radiation resistance of the obtained samples was determined by their irradiation on an electron accelerator with a maximum dose of 10^8 Gy (MPP-Z compound after heat treatment at 180 °C and NAFP glass) and up to 10^9 Gy for a month (ceramics based on bentonite clay), after which the phase composition (XRD) and compressive strength of the samples were investigated.

The hydrolytic stability of the samples obtained was determined in accordance with the semi-dynamic standard GOST R 52126-2003 at 25 ± 3 °C and 90 ± 3 °C [27]. In accordance with the standard, monolithic samples with known open geometric surface area were placed in distilled water used as a leaching agent. Distilled water was periodically replaced after 1, 3, 7, 10, 14, 21 and 28 days. Leaching was carried out in an electrical drying oven 2B-151 (Medlabortehnika, Odessa, Ukraine) in a tightly closed PTFE container. The leached solution was decanted and the content of the components in the solution after leaching was determined by ICP–AES (Agilent 720 (Agilent Technologies Inc., Springvale, Mulgrave, Victoria, Australia) and iCAP-6500 Duo (Thermo Scientific, Waltham, MA, USA)) and ICP–MS (X Series2 (Thermo Scientific, Waltham, MA, USA)), respectively. The ^{137}Cs and ^{152}Eu content in the solution was determined by gamma-ray spectrometry on a spectrometer with a high-purity germanium detector GC 1020 (Canberra, Meriden, CT, USA); ^{239}Pu content in the solution was determined using an α- spectrometer Alpha Analyst (Canberra, Meriden, CT, USA).

The leaching rate LR, [g/(cm^2·day)], of the components was calculated by Equation:

$$LR = \frac{c \cdot V}{S \cdot f \cdot t},$$

where c–element concentration in solution after leaching, g/L; V–the volume of leaching agent, L; S–the sample surface, cm^2; f–element content in matrix, g/g; t–duration of the n-th leaching period between replacements of contact solution, days.

3. Results and Discussion

3.1. Characterization of the Synthesised Compounds Containing Chlorides

The obtained X-ray diffraction patterns of the samples after solidification of spent electrolyte imitator are shown in Figure 1. It was found (Figure 1a) that the main crystalline phase of the MPP compound is the target matrix phase of the composition $MgKPO_4 \cdot 6H_2O$-K-struvite analog (Phase #1, main reflexes at 4.25 and 4.13 Å). The MgO phase (Phase #2, periclase, main reflexes at 2.11 and 2.43 Å), which is associated with an excess of used MgO relative to the stoichiometry of the reaction of the formation of MPP matrix [28], and the $MgHPO_4 \cdot 3H_2O$ phase (Phase #3, newberyite, main reflexes at 3.04 and 3.46 Å), which is formed in the reaction of $Mg(H_2PO_4)_2$ with MgO in water solution [29], are also present in the MPP compound. It was shown that lithium and cesium are present in the compound as components of low-soluble phosphates, for example, cesium-$MgCsPO_4 \cdot 6H_2O$ (Phase #4, main reflexes at 5.40 and 3.44 Å), indicating the replacement of potassium ions with cesium in the matrix structure, while lithium-Li_3PO_4 (Phase #5, lithiophosphate, main reflexes at 3.99 and 3.82 Å). This is confirmed by the presence of the KCl phase (Phase #6, sylvite, main reflexes at 3.15 and 2.23 Å) in the compound, which was also noted earlier in the immobilization of CsCl in the MPP compound [18].

It was found that the NAFP glass samples are homogeneous and amorphous (Figure 1b), which indicates a high resistance of this glass composition to crystallization.

Ceramics based on bentonite clay represent polyphase materials with the following main observed phases (Figure 1c): $KAlSi_3O_8$ (Phase #7, orthoclase, main peaks at 3.31 and 3.77 Å), $LiAlSi_3O_8$ (Phase #8, main peaks at 3.47 and 3.89 Å), $SrAl_2Si_2O_8$ (Phase #9, main peaks at 3.27 and 3.22 Å). Additionally, some minor phases (($Na,K)AlSi_3O_8$, $CsAlSiO_4$, $CsAlSi_2O_6$) can present in the samples as it was shown in [17]. Thus, it can be suggested that fission products (primarily cesium and strontium) enter the crystal lattice of ceramics based on bentonite clay, that improves the immobilization (fixation) of RW in the samples.

SEM micrographs of the surface of the obtained materials containing spent electrolyte imitators are shown in Figure 2. It was noted that the MPP compound consists of several phases, in which elemental composition based on the results of EDS analysis is presented in Table 1. It was found that the main phase consists of the main matrix components Mg, K, and P (Phase #1, Figure 2a, Table 1). Light inclusions contain cesium up to 2.5 at% (Phase #2, Figure 2a, Table 1), which partially replaced potassium in the matrix. The KCl phase (Phase #3, Figure 2a, Table 1) was detected in the sample, which confirms the XRD results (Phase #6, Figure 1a). It was found that the fission products form low soluble phosphate compounds, and there are some particles containing significant amounts of phosphorus and lanthanum of about 21.4 and 10.9 at%, respectively (Phase #4, Figure 2a,b, Table 1).
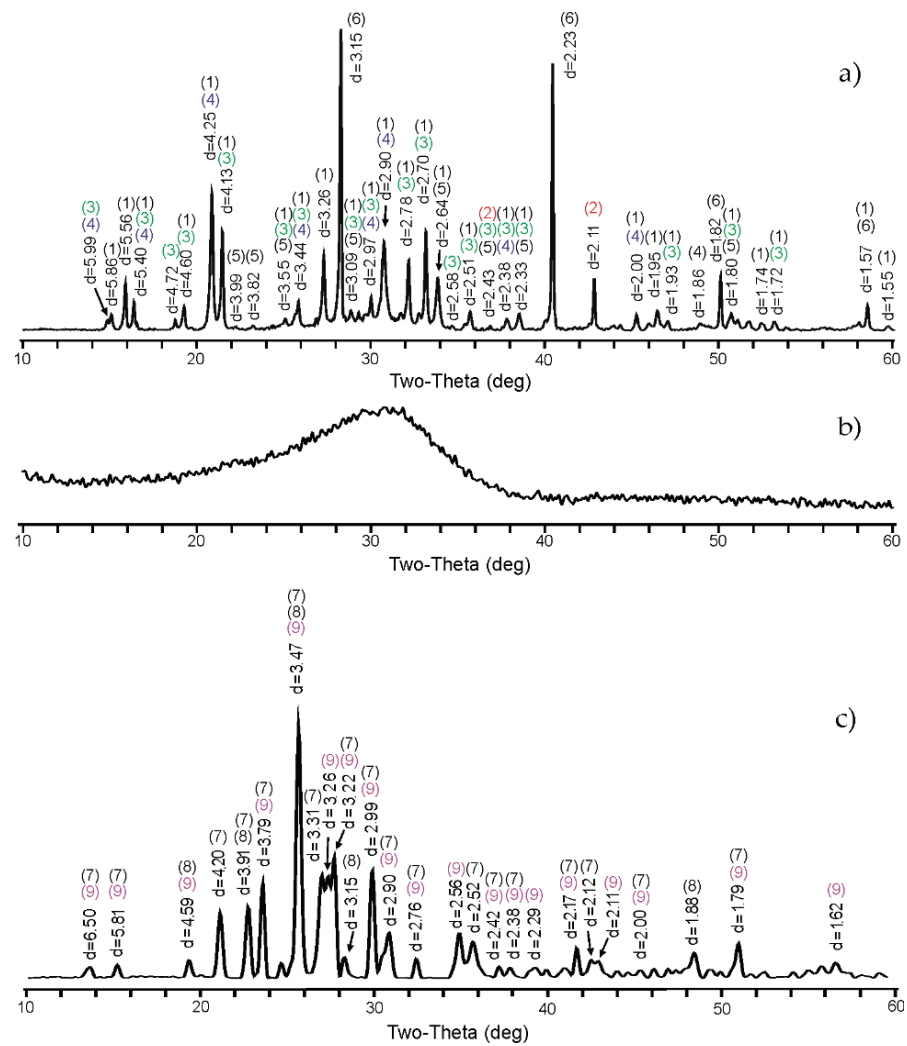
Figure 1. X-ray diffraction patterns of the materials containing spent electrolyte imitator: (**a**) MPP matrix, (**b**) NAFP glass and (**c**) ceramics based on bentonite clay. 1–$MgKPO_4 \cdot 6H_2O$ (K-struvite); 2–MgO (periclase); 3–$MgHPO_4 \cdot 6H_2O$ (newberyite);4–$MgCsPO_4 \cdot 6H_2O$; 5–Li_3PO_4 (lithiophosphate); 6–KCl (sylvite); 7–$KAlSi_3O_8$ (orthoclase); 8–$LiAlSi_3O_8$; 9–$SrAl_2Si_2O_8$.

Crystalline phase formation was not detected on the surface of NAFP glass (Figure 2c), which confirms the XRD results of the glass homogeneity and amorphousness (Figure 1b). The data on the elemental composition of the studied samples are presented in Table 2. It was found that the quenched samples are represented by a glass phase that coincides in composition with the calculated content in terms of the main structure-forming components. The inclusion of silicon oxide up to 1.2 wt% in the composition of the obtained samples was found, which is due to the synthesis of glasses in quartz crucibles. The elemental composition and the degree of chloride inclusion in glasses were confirmed by XRF. It is shown that about 35% of the introduced amount of chlorides is included in the glass composition.

A SEM micrograph of ceramics based on bentonite indicate that the samples are characterized by the alternation of large aggregates 5 . . . 50 μm in size. The sample consists of three main phases found on XRD and pores no larger than 30 μm (Figure 2d).
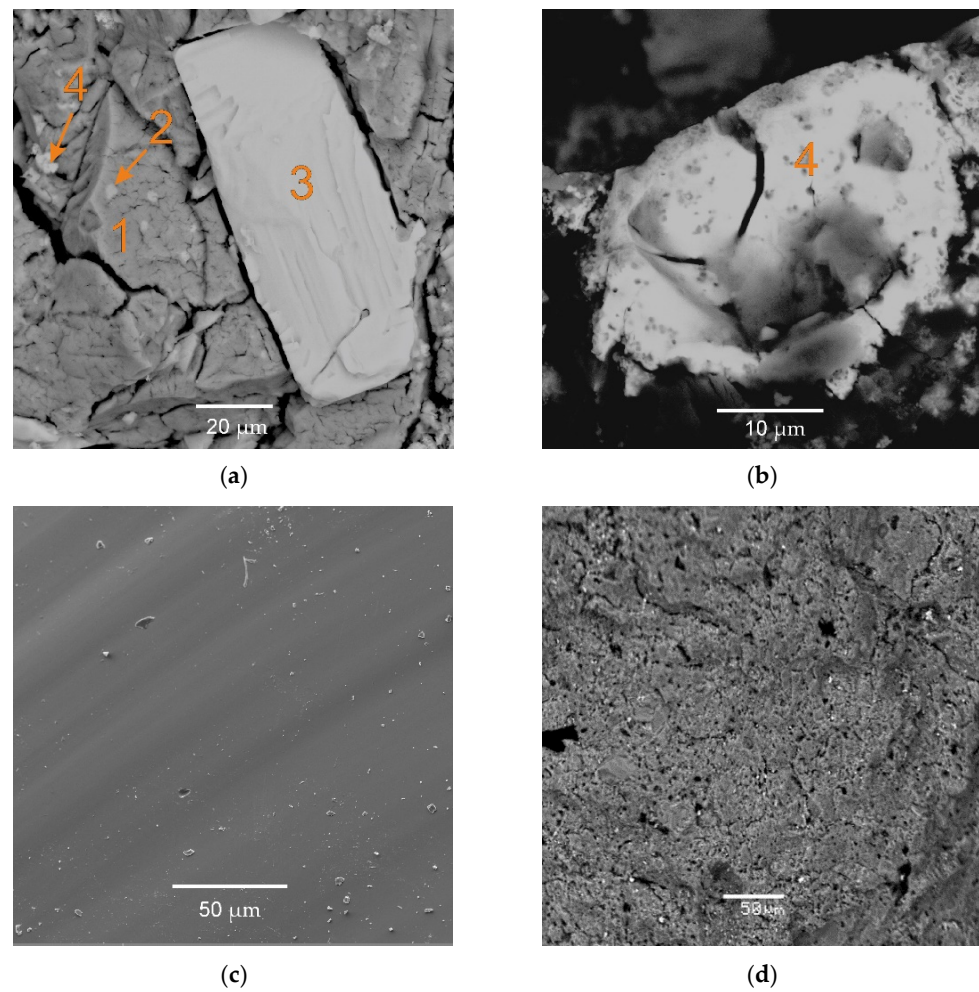
Figure 2. SEM images of the materials containing spent electrolyte imitator: (**a**,**b**) MPP matrix, (**c**) NAFP glass and (**d**) ceramics based on bentonite clay.

Table 1. Average data of elemental composition (at%) of MPP compound containing spent electrolyte imitator according to EDS date.

Element	Phase #1	Phase #2	Phase #3	Phase #4
Mg	16.1	16.2	-	7.9
P	18.0	17.2	-	21.4
K	11.4	8.4	41.0	7.6
Cs	0.1	2.5	-	-
Sr	-	-	-	0.9
Ba	-	-	-	1.0
La	-	-	-	10.9
Cl	0.9	0.8	55.0	3.4
O	53.6	54.8	3.9	46.9

Table 2. The elemental composition (wt%) of NAFP glass samples containing spent electrolyte imitator.

Element	Calculated	SEM-EDS	XRF
Na	15.4	14.2	15.2
P	20.7	21.7	20.1
Fe	9.3	8.7	10.0
Al	4.5	5.4	4.8
Cs	0.3	0.2	0.3
K	1.6	1.8	1.6
Li	0.4	-	-
La	1.7	1.7	2.3
Sr	0.2	0.5	0.4
Ba	0.3	0.3	0.4
Cl	5.4	1.9	1.9
O	40.2	42.4	41.6
Si	-	1.2	1.4

3.2. Mechanical, Thermal and Radiation Resistance of Materials

The results of tests on determination of compressive strength of the MPP compound samples obtained by solidification of electrolyte imitator solution of composition $Li_{0.4}K_{0.28}La_{0.08}Cs_{0.016}Sr_{0.016}Ba_{0.016}Cl$ and containing 23 wt% zeolite are presented in Figure 3. It was established that with increasing the chloride content in the compound the compressive strength of the samples increases by 2–3 times. This parameter reaches about 24 MPa at the maximum chloride content (12 wt%) in the compound. These values are higher than the regulatory requirements for solidified RW (not less than 9 MPa) [26]. It was noted that when 23 wt% zeolite is added to the compound, the compressive strength of the samples increases and is about 40 MPa (Figure 3).
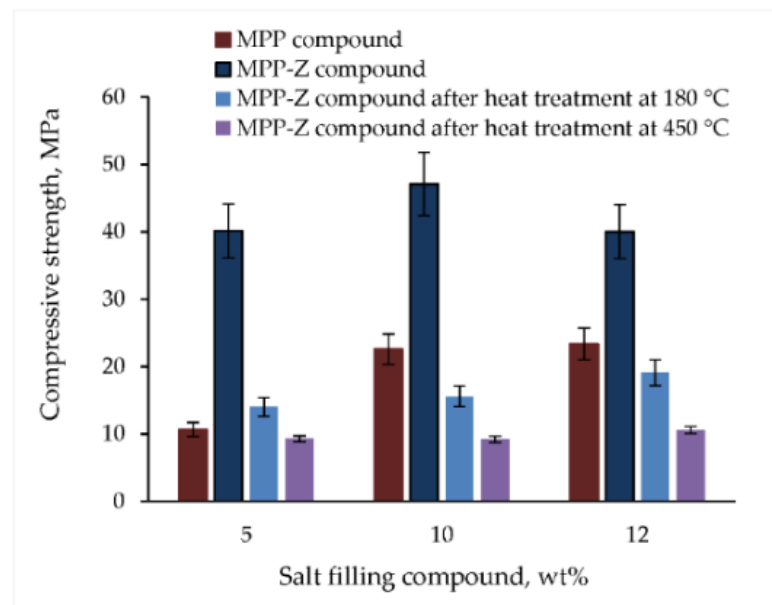
Figure 3. Compressive strength of MPP compound containing spent electrolyte imitator.

To determine the thermal and radiation resistance of the MPP compound with immobilized RW imitator solution, the samples were first heated at 180 °C for 6 h to remove bound water from the compounds. The compressive strength of MPP-Z compound decreases after heat treatment of samples at 450 °C for 4 h. The decrease in the compressive strength of the compound is probably associated with an increase in the porosity of the sample due to the removal of bound water, as shown in [30], and a transformation of the crystalline structure of the MPP compound into an amorphous one, as shown in [31]. It has to be noted that

the compressive strength of the studied compounds meets the regulatory requirements for solidified RW and is not less than 9 MPa (Figure 3) [26]. High values of the compressive strength ensure radiation safety when handling solidified radioactive waste (transportation, reloading, placement in a storage facility). At the same time, zeolite exhibits reinforcing properties, allowing the maintaining of the strength of the compound at the required level, even after high temperature treatment of samples, as was shown earlier in [19].

It was found that the surface of NAFP glass samples after heat treatment at 450 °C for 4 h is inhomogeneous and consists of several phases (Figure 4a). This is probably due to the crystallization process that began on the sample surface, which is characteristic of glasses at (480–630) °C [32]. Several phases with different contents of structure-forming elements (glass phases (Phase #1, Figure 4a, Table 3) and a mixture of sodium–iron–aluminum pyrophosphates (Phase #2, Figure 4a, Table 3), as shown earlier in [22]) as well as a phase containing sodium and chlorine (Phase #3, Figure 4a, Table 3) were found. The transition zone of degradation of the surface of NAFP glass is shown in Figure 4b, the thickness of the altered surface layer was about 2–3 microns.

(a) (b)
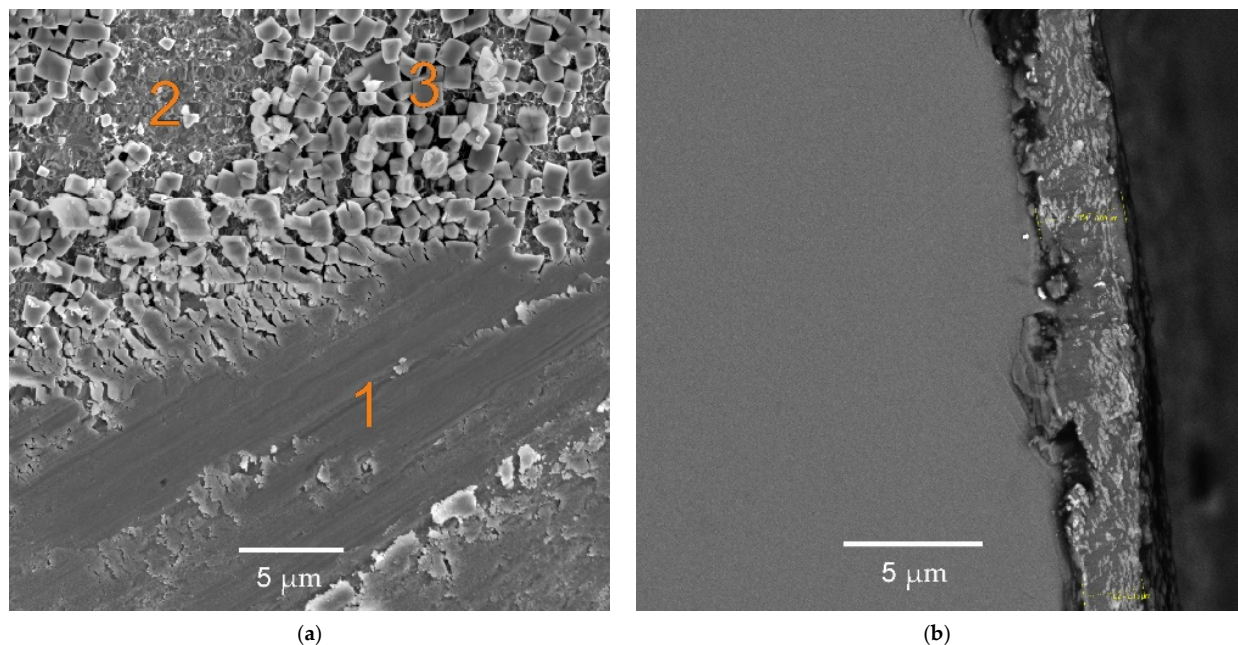
Figure 4. SEM image of (**a**) NAFP glass and (**b**) cleavage surface of the sample after heat treatment at 450 °C.

Table 3. The elemental composition (wt%) of NAFP glass after heat treatment at 450 °C.

| Element	Phase #1	Phase #2	Phase #3
Na	5.2	1.6	30.1
P	24.3	19.7	5.5
Fe	13.5	27.8	6.2
Al	4.7	3.7	0.9
K	2.1	2.2	-
Cs	0.4	0.3	0.2
La	2.5	3.1	0.8
Sr	0.3	0.3	0.1
Ba	0.6	0.6	0.4
Cl	2.1	0.4	35.0
O	43.4	39.4	20.6
Si	1.0	1.0	0.3

The data on the compressive strength of the ceramics based on bentonite clay, including after heat treatment at 450 °C for 4 h and irradiation by electrons, are presented in

Table 4. It is shown that all samples have a high compressive strength of about 40–50 MPa and comply with the regulatory requirements for immobilized HLW (at least 9 MPa) [26].

Table 4. Compressive strength of ceramics based on bentonite clay during thermal and radiation tests.

Samples	Test Parameters	Compressive Strength, MPa
Initial sample	-	51.3 ± 7.3
After thermal tests	Thermal treatment at 450 °C	50.9 ± 6.9
After irradiation tests (irradiation by electrons)	10^7 Gy	41.5 ± 8.4
	10^8 Gy	48.3 ± 6.8
	10^9 Gy	39.9 ± 5.7

Radiation stability is one of the important characteristics of solidified radioactive waste, which is characterized, first of all, by the stability of the structure of the samples. Electron irradiation of samples is used to simulate beta decay of fission products [33]. It was found that the phase composition of samples of the MPP-Z compound, NAFP glass and ceramics based on bentonite clay after their electron irradiation remained stable, the diffractograms of original samples of the studied compounds and after their irradiation are identical (Figures 5 and 6). Thus, the MPP-Z compound after its dehydration (Figure 5) consists of the same phases as in the original sample: the KCl phase and the main mineral phases of zeolite (Phase #1, clinoptilolite-Na and Phase #2, heulandite) and quartz (Phase #3) contained in zeolite (74% and 12%, respectively [19]). At the same time, for ceramics based on bentonite clay (Figure 6), only a relatively small broadening of the peaks and an insignificant change in the relative content of minor mineral phases were observed, but, most likely, this is due to the heterogeneity of the samples. Thus, the observed stability of the studied materials at absorbed doses of 10^8–10^9 Gy allows one to predict the stability of solidified forms of RW for at least 10,000 years of storage [26].
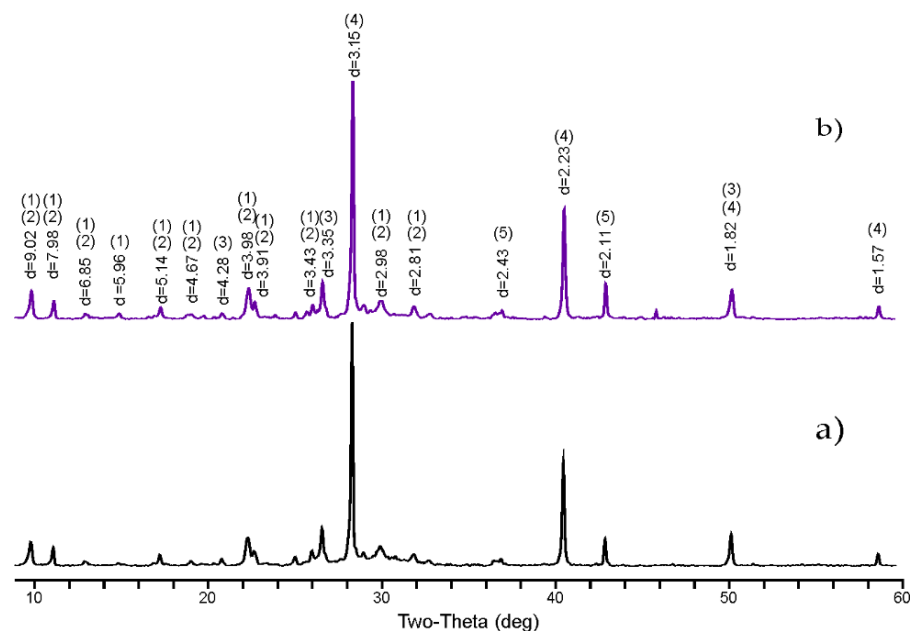
Figure 5. X-ray diffraction patterns of the (**a**) MPP-Z compound, including (**b**) after irradiation up to 10^8 Gy. 1–$(Na, K, Ca)_5Al_6Si_{30}O_{72} \cdot 18H_2O$ (clinoptilolite-Na); 2–$Ca_{3.6}K_{0.8}Al_{8.8}Si_{27.4}O_{72} \cdot 26.1H_2O$ (heulanditea); 3–SiO_2 (quartz); 4–KCl (sylvite); 5–MgO (pereclase).
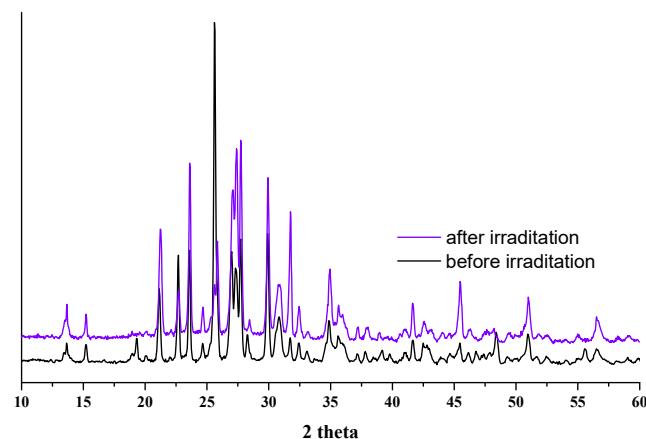
Figure 6. X-ray diffraction patterns of the ceramics based on bentonite clay, including after irradiation up to 10^9 Gy.

3.3. Hydrolytic Resistance of the Materials

The obtained data on the differential leaching rate of waste components from MPP-Z compound samples, including after heat treatment up to 450 °C, are shown in Figure 7. The leaching rates of Sr, La and Ba reduced by two orders of magnitude after the thermal treatment of the compound at 450 °C and equal to 1.6×10^{-7}, 3.0×10^{-7} and 2.3×10^{-6} g/(cm^2·day), respectively, at 28th days of contact with water (Figure 7a). The differential leaching rate of ^{137}Cs and ^{152}Eu (Figure 7b,c, respectively) from all samples under study on the 28th day of contact of the samples with water was about 10^{-5} g/(cm^2·day), and ^{239}Pu (Figure 7d) was about 10^{-6} g/(cm^2·day), which is close to the normative requirements for vitrified HLW (no more than 1.0×10^{-5} g/(cm^2·day) for ^{137}Cs and 1.0×10^{-7} g/(cm^2·day) for ^{239}Pu) [26]. The heat treatment up to 450 °C of the compounds does not lead to a significant change in leaching rate.

The kinetic dependences of sodium leaching rate from NAFP glass are presented in Figure 8a. It should be noted that there are no normative requirements for sodium leaching rate from solidified HLW, but due to the similarity of chemical behavior of sodium and cesium, it is possible to be oriented on norms for cesium: ^{137}Cs leaching rate from glass-like compounds should not exceed 10^{-5} g/(cm^2·day) [26]. The data in Figure 8a show that the differential sodium leaching rate is about 10^{-6} g/(cm^2·day), which meets the normative requirements, including after the glass heat treatment at 450 °C. It was found that the ^{137}Cs and ^{152}Eu contents in the solutions after leaching of NAFP samples were below detection limits, indicating high water resistance of NAFP glass to leaching of the most mobile nuclides. The differential leaching rate of ^{239}Pu from NAFP glass upon sample leaching at 25 °C on the 7th day of contact with water is no more than 4.8×10^{-8} g/(cm^2·day) and the content of ^{239}Pu in solutions during the test was below the detection limits. At the same time, the leaching of ^{239}Pu from glass samples at 90 °C is observed, so the differential leaching rate from NAFP glass after heat treatment at 450 °C is higher than that from the original glass samples (Figure 8b). It is likely that the increased leaching of ^{239}Pu is due to its leaching from the formed modified surface layer (Figure 4). At the same time, the leaching rate of ^{239}Pu decreases to 4.7×10^{-7} g/(cm^2·day) on the 28th day of water contact after the sample was exposed to heat treatment at 450 °C, which is close to the normative requirements for vitrified HLW (no more than 10^{-7} g/(cm^2·day)) [26] and is likely to reach the required value when the tests continue.
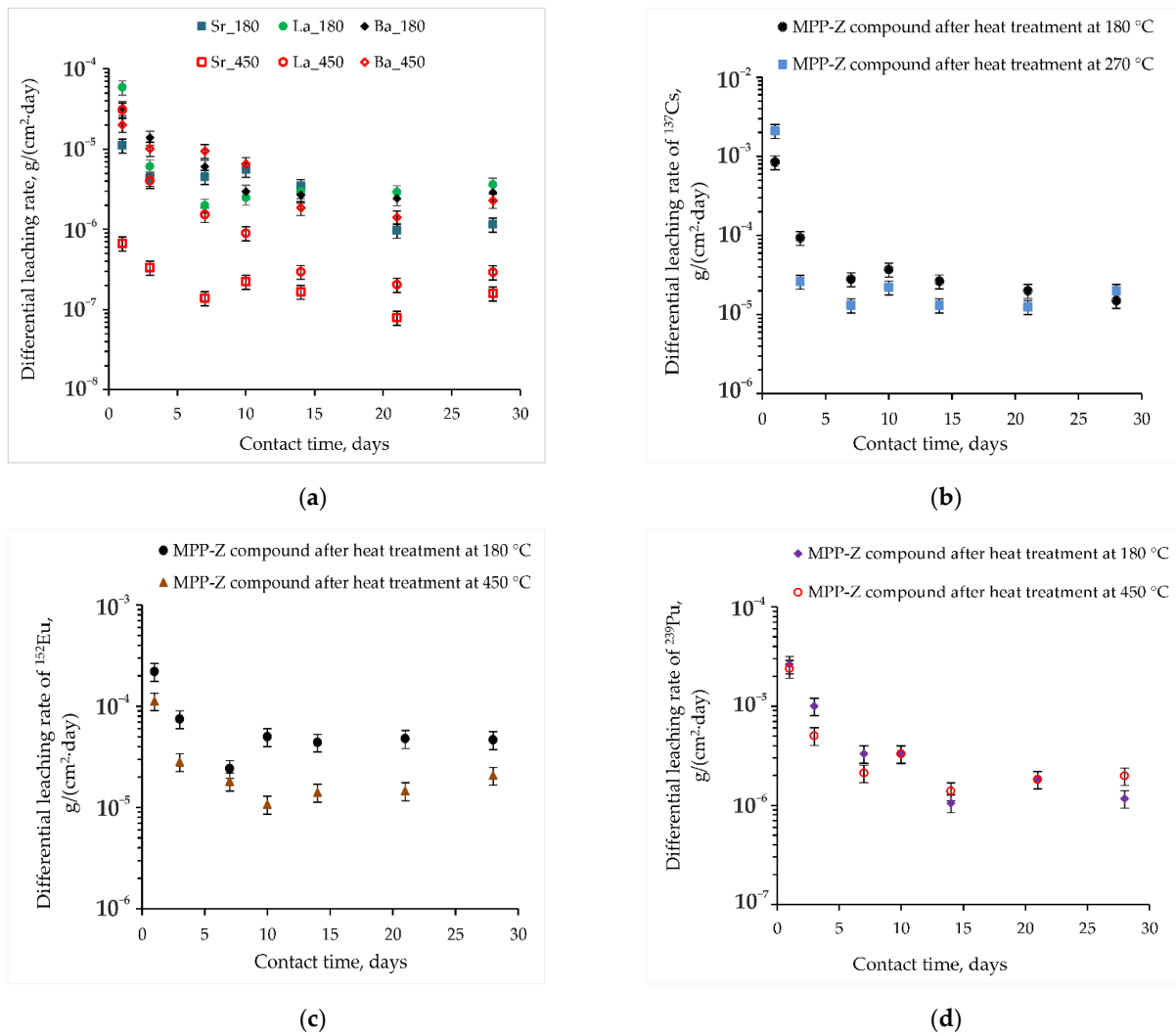
Figure 7. Kinetic curve of the leaching rate of (**a**) of the solidifying waste imitator components (**b**) ^{137}Cs, (**c**)^{152}Eu and (**d**) ^{239}Pu from MPP-Z compound, including after its heat treatment.
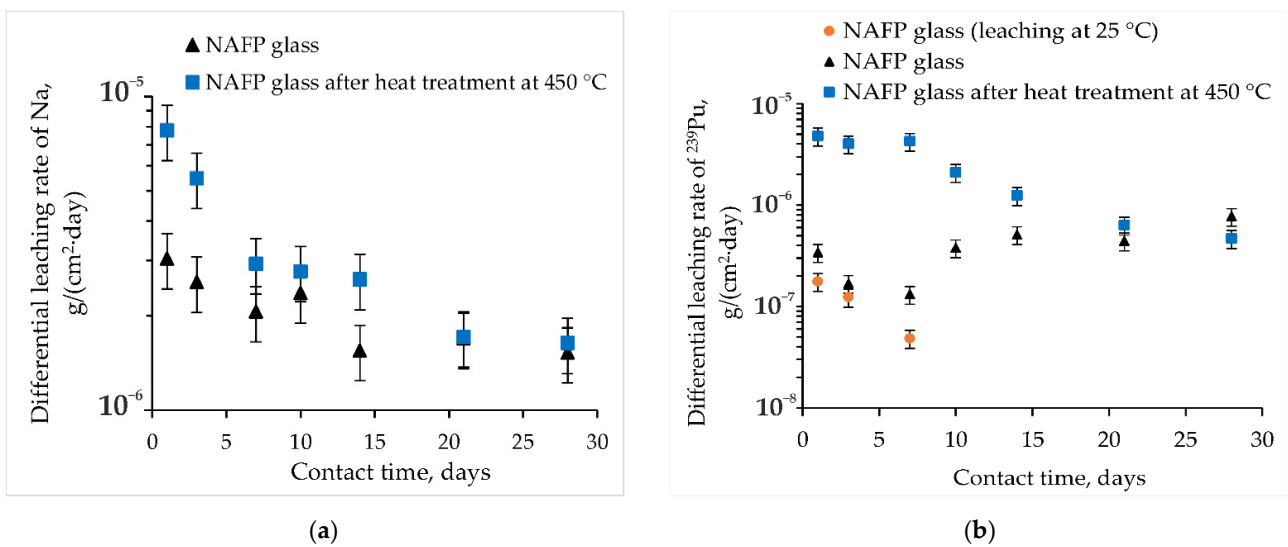
Figure 8. Kinetic curve of the leaching rate of (**a**) sodium and (**b**) plutonium from NAFP glass.

Figure 9 shows the kinetic curves of the differential leaching rate of components from ceramic samples based on bentonite clay. The leaching rate of cesium, as one of the main components of waste, from the samples is about 3×10^{-5} g/(cm^2·day), which is close to the regulatory requirements for immobilized HLW [26]. It may also be noted that the leaching rate on the 28th day of the main elements of the sample is quite low for all the samples studied, which confirms their hydrolytic stability.
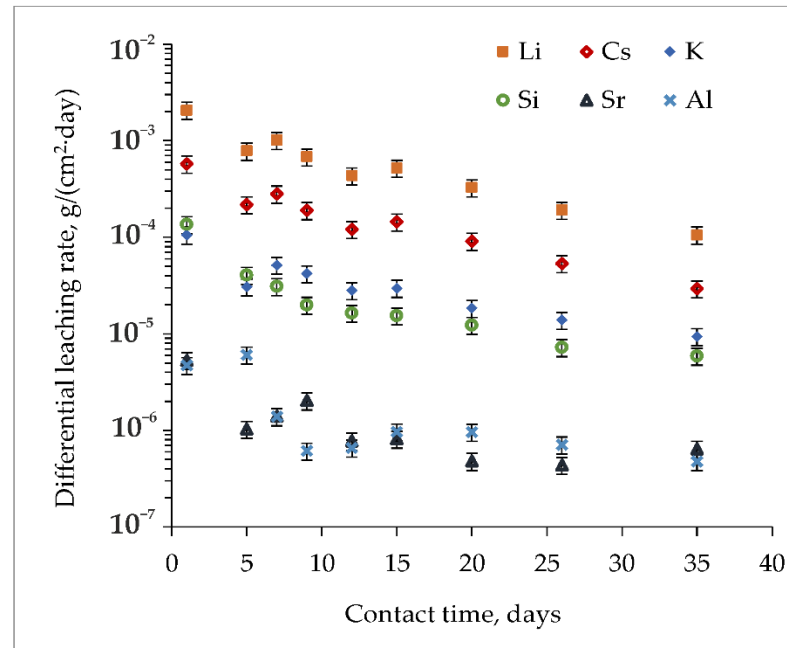
Figure 9. Kinetic curve of the leaching rate of components of the ceramics based on bentonite clay.

4. Conclusions

In this work, three types of matrices (MPP matrix, NAFP glass, ceramics based on natural bentonite clay) with the addition up to 20 wt% of the spent electrolyte imitator LiCl-KCl were synthesized. The phase composition of the samples, their mechanical, hydrolytic, thermal and radiation stability were characterized. The results of this work indicate that the studied matrices and methods of their synthesis provide reliable characteristics that comply with the regulated requirements for immobilized RW: mechanical compressive strength ≥ 9 MPa; radiation resistance (without changes in mechanical strength and structure at an absorbed dose of up to 10^8–10^9 Gy); and leaching rate (for all components $\leq 10^{-5}$ g/(cm^2·day)).

Each of the materials has its own advantages and individual disadvantages. Thus, a low-temperature MPP matrix is easily synthesized at room temperature, but its strength is dramatically decreased under thermal stress. The glass forms a homogeneous system, demonstrates low leaching rates, but under thermal loads, the release of individual mineral phases on the surface is observed. A ceramic matrix based on bentonite clay is able to withstand both thermal loads and high doses of radiation, but the method for synthesizing such a matrix requires complex operations.

As the result, the fundamental possibility to immobilize and include up to 20 wt% HLW from pyrochemical processing of MNUP SNF into the matrix was confirmed. The choice of the optimal matrix depends on the final option of the technology for purifying the electrolyte from radionuclides. Different options will result in generation of RW of various levels of radiation hazard; therefore, it will determine methods of their immobilization. In the case of intermediate level waste and, accordingly, a low probability of radiation heating produced by immobilized radionuclides, the MPP matrix seems to be optimal, while both glass and bentonite ceramics are promising for HLW.

Further investigations will be aimed at testing various modifiers for the studied matrices, which would improve their characteristics.

Conflicts of Interest: The authors declare no conflict of interest. The funders had no role in the design of the study; in the collection, analyses, or interpretation of data; in the writing of the manuscript, or in the decision to publish the results.

References

1. Shadrin, A.Y.; Dvoeglazov, K.N.; Maslennikov, A.G.; Kashcheev, V.A.; Tret'yakova, S.G.; Shmidt, O.V.; Vidanov, V.L.; Ustinov, O.A.; Volk, V.I.; Veselov, S.N.; et al. PH process as a technology for reprocessing mixed uranium–plutonium fuel from BREST-OD-300 reactor. *Radiochemistry* **2016**, *58*, 271–279. [CrossRef]
2. Poluektov, P.P.; Schmidt, O.V.; Kascheev, V.A.; Ojovan, M.I. Modelling aqueous corrosion of nuclear waste phosphate glass. *J. Nucl. Mater.* **2017**, *484*, 357–366. [CrossRef]
3. Choi, J.; Um, W.; Choung, S. Development of iron phosphate ceramic waste form to immobilize radioactive waste solution. *J. Nucl. Mater.* **2014**, *452*, 16–23. [CrossRef]
4. Donald, I.W.; Metcalfe, B.L.; Fong, S.K.; Gerrard, L.A.; Strachan, D.M.; Scheele, R.D. A glass-encapsulated calcium phosphate wasteform for the immobilization of actinide-, fluoride-, and chloride-containing radioactive wastes from the pyrochemical reprocessing of plutonium metal. *J. Nucl. Mater.* **2007**, *361*, 78–93. [CrossRef]
5. Pereira, C.; Hash, M.; Lewis, M.; Richmann, M. Ceramic-composite waste forms from the electrometallurgical treatment of spent nuclear fuel. *JOM* **1997**, *49*, 34–40. [CrossRef]
6. Morrison, M.C.; Bateman, K.J.; Simpson, M.F. Scale Up of Ceramic Waste Forms for the EBR-II Spent Fuel Treatment Process. In *Office of Scientific and Technical Information Technical Reports*; Idaho National Laboratory: Idaho Falls, ID, USA, 2010; pp. 1–17.
7. Priebe, S.; Bateman, K. The Ceramic Waste Form Process at Idaho National Laboratory. *Nucl. Technol.* **2008**, *162*, 199–207. [CrossRef]
8. Kuzin, M.A.; Makarov, A.O. Study of sorption properties of lithium and potassium inoculated NaA zeolite sorbent. *Ecol. Ind. Russ.* **2015**, *19*, 8–11. [CrossRef]
9. Tomilin, S.V.; Lukinykh, A.N.; Lizin, A.A.; Bychkov, A.V.; Yakovlev, V.V.; Konovalov, V.I. Investigation of the incorporation of spent alkali chloride melt in ceramic. *At. Energy* **2007**, *102*, 217–222. [CrossRef]
10. Park, H.S.; Ahn, B.-G.; Kim, H.-Y.; Kim, I.-T.; Cho, Y.-Z.; Lee, H. Solidification Method of Radioactive Waste Accompanying Chloride Recycling or Radioactive Iodide Removing and the Device Thereof. U.S. Patent No. 9,087,618 B2, 21 July 2015.
11. Lee, K.R.; Riley, B.J.; Park, H.-S.; Choi, J.-H.; Han, S.Y.; Hur, J.-M.; Peterson, J.A.; Zhu, Z.; Schreiber, D.K.; Kruska, K.; et al. Investigation of physical and chemical properties for upgraded SAP (SiO2Al2O3P2O5) waste form to immobilize radioactive waste salt. *J. Nucl. Mater.* **2019**, *515*, 382–391. [CrossRef]
12. Ringwood, A.E. *Safe Disposal of High Level Nuclear Reactor Wastes: A New Strategy*, 1st ed.; Australian National University Press: Canberra, Australia, 1978; pp. 1–63.

13. Ringwood, A.E.; Oversby, V.M.; Kesson, S.E.; Sinclair, W.; Ware, N.; Hibberson, W.; Major, A. Immobilization of high-level nuclear reactor wastes in SYNROC: A current appraisal. *Nucl. Chem. Waste Manag.* **1981**, *2*, 287–305. [CrossRef]
14. Lizin, A.A.; Tomilin, S.V.; Gnevashov, O.E.; Lukinykh, A.N.; Orlova, A.I. Orthophosphates of langbeinite structure for immobilization of alkali metal cations of salt wastes from pyrochemical processes. *Radiochemistry* **2012**, *54*, 542–548. [CrossRef]
15. Laverov, N.P.; Yudintsev, S.V.; Stefanovsky, S.V.; Omel'yanenko, B.I.; Nikonov, B.S. Murataite as a universal matrix for immobilization of actinides. *Geol. Ore Deposits* **2006**, *48*, 335–356. [CrossRef]
16. Lizin, A.A.; Tomilin, S.V.; Poglyad, S.S.; Pryzhevskaya, E.A.; Yudintsev, S.V.; Stefanovsky, S.V. Murataite: A matrix for immobilizing waste generated in radiochemical reprocessing of spent nuclear fuel. *J. Radioanal. Nucl. Chem.* **2018**, *318*, 2363–2372. [CrossRef]
17. Matveenko, A.V.; Varlakov, A.P.; Zherebtsov, A.A.; Germanov, A.V.; Mikheev, I.V.; Kalmykov, S.N.; Petrov, V.G. Natural Clay Minerals as a Starting Material for Matrices for the Immobilization of Radioactive Waste from Pyrochemical Processing of SNF. *Sustainability* **2021**, *13*, 10780. [CrossRef]
18. Kulikova, S.A.; Belova, K.Y.; Tyupina, E.A.; Vinokurov, S.E. Conditioning of Spent Electrolyte Surrogate LiCl-KCl-CsCl Using Magnesium Potassium Phosphate Compound. *Energies* **2020**, *13*, 1963. [CrossRef]
19. Kulikova, S.A.; Vinokurov, S.E. The Influence of Zeolite (Sokyrnytsya Deposit) on the Physical and Chemical Resistance of a Magnesium Potassium Phosphate Compound for the Immobilization of High-Level Waste. *Molecules* **2019**, *24*, 3421. [CrossRef]
20. Kulikova, S.A.; Danilov, S.S.; Belova, K.Y.; Rodionova, A.A.; Vinokurov, S.E. Optimization of the Solidification Method of High-Level Waste for Increasing the Thermal Stability of the Magnesium Potassium Phosphate Compound. *Energies* **2020**, *13*, 3789. [CrossRef]
21. Vance, E.R.; Davis, J.; Olufson, K.; Chironi, I.; Karatchevtseva, I.; Farnan, I. Candidate waste forms for immobilisation of waste chloride salt from pyroprocessing of spent nuclear fuel. *J. Nucl. Mater.* **2012**, *420*, 396–404. [CrossRef]
22. Stefanovsky, S.V.; Stefanovskaya, O.I.; Vinokurov, S.E.; Danilov, S.S.; Myasoedov, B.F. Phase composition, structure, and hydrolytic durability of glasses in the Na_2O-Al_2O_3-(Fe_2O_3)-P_2O_5 system at replacement of Al_2O_3 by Fe_2O_3. *Radiochemistry* **2015**, *57*, 348–355. [CrossRef]
23. Stefanovskii, S.V.; Stefanovskaya, O.I.; Semenova, D.V.; Kadyko, M.I.; Danilov, S.S. Phase Composition, Structure, and Hydrolytic Stability of Sodium-Aluminum(Iron) Phosphate Glass Containing Rare-Earth Oxides. *Glas. Ceram.* **2018**, *75*, 89–94. [CrossRef]
24. Maslakov, K.I.; Teterin, Y.A.; Stefanovsky, S.V.; Kalmykov, S.N.; Teterin, A.Y.; Ivanov, K.E.; Danilov, S.S. XPS study of neptunium and plutonium doped iron-bearing and iron-free sodium-aluminum-phosphate glasses. *J. Non-Cryst. Solids* **2018**, *482*, 23–29. [CrossRef]
25. Belousov, P.E.; Krupskaya, V.V.; Zakusin, S.V.; Zhigarev, V.V. Bentonite clays from 10th khutor deposite: Features of genesis, composition and adsorption properties. *Rudn J. Eng. Res.* **2017**, *18*, 135–143. [CrossRef]
26. NP-019-15. *Federal Norms and Rules in the Field of Atomic Energy Use "Collection, Processing, Storage and Conditioning of Liquid Radioactive Waste. Safety Requirements"*; With Changes (Order No. 299 Dated 13.09.2021); Rostekhnadzor: Moscow, Russia, 2015; pp. 1–22.
27. GOST R 52126-2003. *Radioactive Waste. Long Time Leach Testing of Solidified Radioactive Waste Forms*; Gosstandart 305: Moscow, Russia, 2003; pp. 1–8.
28. Vinokurov, S.E.; Kulikova, S.A.; Krupskaya, V.V.; Myasoedov, B.F. Magnesium Potassium Phosphate Compound for Radioactive Waste Immobilization: Phase Composition, Structure, and Physicochemical and Hydrolytic Durability. *Radiochemistry* **2018**, *60*, 70–78. [CrossRef]
29. Wagh, A.S. *Chemically Bonded Phosphate Ceramics: Twenty-First Century Materials with Diverse Applications*, 2nd ed.; Elsevier: Amsterdam, The Netherlands, 2016; pp. 1–422. ISBN 978-0-08-100380-0.
30. Fu, M.; Yang, H.; Wu, C.; Ying, Z.; You, C.; Qian, J. Effects of Temperature on the Properties of α-High-level Radioactive Waste Immobilized, Hardened Magnesium Phosphate Cement. *Cailiao Daobao/Mater. Rev.* **2017**, *31*, 86–90. [CrossRef]
31. Gardner, L.J.; Walling, S.A.; Lawson, S.M.; Sun, S.; Bernal, S.A.; Corkhill, C.L.; Provis, J.L.; Apperley, D.C.; Iuga, D.; Hanna, J.V.; et al. Characterization of and Structural Insight into Struvite-K, $MgKPO_4 \cdot 6H_2O$, an Analogue of Struvite. *Inorg. Chem.* **2021**, *60*, 195–205. [CrossRef] [PubMed]
32. Doupovec, J.; Sitek, J.; Kákoš, J. Crystallization of iron phosphate glasses. *J. Therm. Anal.* **1981**, *22*, 213–219. [CrossRef]
33. Weber, W.J. Radiation and Thermal Ageing of Nuclear Waste Glass. *Procedia Mater. Sci.* **2014**, *7*, 237–246. [CrossRef]